CHEMICAL ENGINEERING TRANSACTIONS Volume 24, 2011
Editor Sauro Pierucci
Copyright © 2011, AIDIC Servizi S.r.l., ISBN 978-88-95608-15-0 ISSN 1974-9791
DOI: 10.3303/CET1124036

Production of Nanoparticles of Hydroxyapatite by Using a Rotating Disk Reactor

Mariapaola Parisi *, Marco Stoller, Angelo Chianese

University of Rome "La Sapienza", Dept. of Chemical Engineering, Via Eudossiana 18, 00184 Rome, Italy.
mariapaola.parisi@uniroma1.it

This paper deals with the feasibility to produce, in a continuous mode, nanoparticles of hydroxyapatite (HAP) by means of a rotating disk reactor. This device is capable to establish the required conditions of micromixing in correspondence of the reagents feeding point. The experimental work consists mainly of investigating the effect of the feed location of the reagents over the rotating disk surface. It was observed a great influence of the feed location on the particle size distribution of the produced HAP, only the best feed location allow the production of particles smaller than 100 nanometers.
The obtained experimental results were interpreted on the light of a simplified simulation model. The model provided the map of the specific dispersed energy, thus allowing identifying the zones of the disk where micromixing may occur.

1. Introduction

Hydroxyapatite (HAP) and β-tricalcium phosphate (β-TCP) ceramics have been widely used as bone graft in spine and orthopedic surgery and dentistry. These ceramics exhibited highly biocompatible properties and osteo-conductivity, as demonstrated by several authors. Balasundaram et. al (2006) showed that decreasing the particles size into the nanometer range may promote osteoblast adhesion. HAP is usually produced by a reaction-precipitation process performed by means of a stirring vessel provided by a turbine impeller. This latter apparatus leads to the production of HAP particles several hundreds of nanometers in size.
The main aim of this study is to suggest the use of a Rotating Disk Reactor (RDR) to make the synthesis and precipitation of HAP as a unique apparatus to produce nanoparticles of HAP at industrial level. In fact this intensification process apparatus, as reported by Cafiero et al. (2002) may provide micromixing of the reagents solution over the disk surface at reasonable values of specific dispersed energy. In a previous work, Stoller et al. (2009) pointed out the importance to determine optimal feed location of the reagents on the rotating disk surface in order to achieve the best results. Therefore, the first step in this work was to determine the optimal feed location of the reagents to produce HAP nanoparticles smaller than 100 nm.

Please cite this article as: Parisi M., Stoller M. and Chianese A., 2011, Production of nanoparticles of hydroxyapatite by using a rotating disk reactor, Chemical Engineering Transactions, 24, 211-216
DOI: 10.3303/CET1124036

Moreover, the obtained results were justified by a simplified simulation model, developed to evaluate the map of the specific dispersed energy over the disk, which is related on the degree of intensification of mixing process between the reagents.

2. Experimental Setup

The production process of the HAP nanoparticles consisted of the reaction between two aqueous solutions of calcium chloride and ammonia orthophosphate at 50 °C and the subsequent precipitation of the produced HAP. The adopted apparatus is equipped with a disk of 50 mm of diameter rotating at 1500 rpm. The two reagent solutions were separately fed at the same distance r_{in} from the centre of the disk (see Fig. 1). The feed flow rate of both the reagent solutions was equal to 100 ml/min. A pH value of the overall solution greater than 10 was provided by the injection at the centre of the disk of an aqueous solution of ammonium hydroxide at a flow rate of 80 ml/min. The ratio between the two reagents were strictly maintained at the stechiometric value equal to 1,67. In order to achieve a high degree of purity for the HAP produced material, the obtained particles were carefully washed with water.

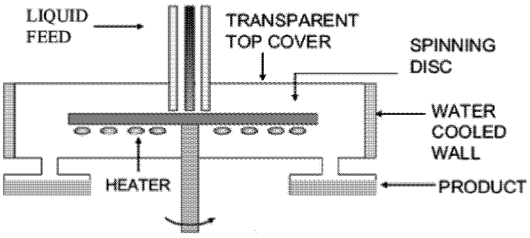

Figure 1: Scheme of the adopted rotating disk reactor.

The purity of the produced HAP was evaluated by an IR analysis, whereas the particle size distribution was measured by the dynamic light scattering technique by using the instrument PLUS 90 supplied by Brookhaven.

3. The RDR's hydrodynamic model

3.1 The hydrodynamic model

The liquid flow over the surface of a rotating disk can be described by the Navier-Stokes equations for incompressible fluids of constant density in a cylindrical co-ordinate system, r, θ and z (Bird et al., 1960). The model can be substantially simplified by the following assumptions (Moore, 1996): the liquid flow is at steady state, the influence of the gravity force is negligible when compared to the effect of the centrifugal force, Coriolis forces are negligible, the effects of the surface tension and shear stress on the liquid free surface are negligible, there is symmetry around the θ axis, the pressure is uniform, the flow regime is laminar and due to the small thickness of the film, the component of the velocity along the z axis is negligible when compared to the components along r and θ. For the same reason, ∂/∂z >> ∂/∂r. On the basis of the above mentioned hypotheses the hydrodynamics can be expressed by means of the balance between the centrifugal force and the opposing viscous forces:

$$- (v^2_\theta / r) = \nu \, (\partial^2 v_r / \partial z^2) \qquad (1)$$

where v_r and v_θ are the velocity components along the co-ordinates r and θ and ν is the kinematic viscosity. Moreover, the velocity components along the θ co-ordinate of the liquid and the disk are the same, thus:

$$v_\theta = \omega \, r \qquad (2)$$

where ω is the radial velocity, and, combining eqs. (1) and (2):

$$- \omega^2 \, r = \nu \, (\partial^2 v_r / \partial z^2) \qquad (3)$$

The integration of eq. (3) with the boundary conditions:

$$v_r = 0 \qquad \text{for } z = 0 \qquad (4)$$
$$(\partial v_r / \partial z) = 0 \qquad \text{for } z = \delta \qquad (5)$$

where δ is the film thickness, leads to the following expressions for the mean velocity radial component:

$$\overline{v}_r = \frac{1}{\delta} \cdot \int_0^\delta v_r dz = \frac{\varpi^2 \cdot r \cdot \delta^2}{3 \cdot \nu} \qquad (6)$$

Due to the steady state hypothesis and the incompressibility of the fluid, the mass balance can be expressed by the following equation:

$$Q = \overline{v}_r \cdot 2\pi r \cdot \delta \qquad (7)$$

where Q is the liquid flow rate. From the eqs. (6) and (7), it follows:

$$\delta = \left(3 / 2\pi \cdot \nu \cdot Q / (\varpi r)^2\right)^{1/3} \qquad (8)$$

The liquid residence time and the specific dispersed power in a volume of the layer delimited by two generic radial co-ordinates, r_a and r_b, can be computed by the following equations (Cafiero et al., 2002), respectively:

$$\tau_{a,b} = \left(\frac{81 \cdot \pi^2 \cdot \nu}{16 \cdot \varpi^2 \cdot Q^2}\right)^{1/3} \cdot \left(r_b^{4/3} - r_a^{4/3}\right) \qquad (9)$$

$$\varepsilon_{a,b} = \frac{1}{2 \cdot \tau_{a,b}} \cdot \left[\left(r^2 \cdot \omega^2 - \overline{v}_r^2\right)_{r=r_b} - \left(r^2 \cdot \omega^2 - \overline{v}_r^2\right)_{r=r_a}\right] \qquad (10)$$

The specific dispersed power determines the micromixing scale length:

$$\lambda = (\nu^3 / \varepsilon)^{1/4} \qquad (11)$$

and, according to Baldyga and Bourne (1984) the micromixing time may be estimated, on first approximation, as:

$$t_{mix} = 12 \cdot (\nu / \varepsilon)^{1/2} \qquad (12)$$

According to Brauer (1958), for any radial co-ordinate r, the liquid layer surface condition can be determined on the basis of Reynold number:

$$Re = Q\,(2\,\pi\, r\, \nu)^{-1} \qquad (13)$$

the flow conditions are: smooth laminar for $Re<4$; lightly waved laminar for $4<Re<10$: waved laminar for $10<Re<20$; turbulent for $Re>20$.

3.2 Effect of the hydrodynamic conditions on the PSD

It is well known that, in a precipitation process, a fast micromixing leads to a uniform size of the produced particles (Cafiero et al.2002): since the mixing time decreases as the specific power ε increases, the injection of the second reagent should be accomplished where ε reaches its maximum. In Fig. 2 the specific dispersed power of the overall feed Vs the radius of the disk for the adopted operating conditions is reported.

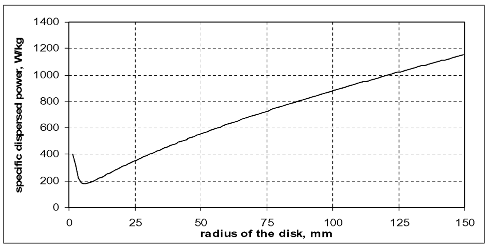

Figure 2: specific dispersed power vs disk radius

From Fig. 2 it appears evident that the injection of the reagents should be accomplished as close to the disk border as possible. On the other hand when there is some residual supersaturation (that is, immediately after the nucleation occurrence), nanoparticles tend to aggregate: during this process it is important to avoid the formation of crystalline bridges among the particles by means of high velocity and turbulence. For these reasons, the reagents should be injected in the inner part of the disk.
Another aspect that may have an influence on the precipitation process is the liquid layer surface condition in the injection point: it is plausible that the presence of waves on the surface may improve the mixing. The above considerations together with the specific energy map in Fig. 2 may be helpful to interpret the experimental results.

4. Results and Discussion

In order to determine the optimal injection point of the reagents, some experiments were carried out on the RDR by changing the distance r_{in} of both reagent injection points at a constancy of the other operating conditions, reported in the paragraph 3 of this paper.
The obtained mean particle diameters, d, are reported in Table 1.

Table 1:Experimental results and hydrodynamic parameters for the RDR runs

run ID	r_{in}	d	$\delta_{1,2}$	$Re_{1,2}$	$\varepsilon_{1,2}$	τ	t_{mix}	$\bar{v}_{1,2}$	λ
	mm	nm	μm	#	W/kg	s	ms	m/s	μm
1	20	79.8	29	10.6	296	0.338	0.20	0.62	7.62
2	30	57.9	22	7.1	390	0.321	0.18	0.54	7.12
3	50	171.1	16	4.2	559	0.278	0.15	0.45	6.50

The smallest particles are obtained when r_{in} is equal to 30 mm, that is very close to the centre of the disc. This is the same result, reported previously by Stoller et al. (2009), by using the same RDR for the production of TiO_2 nanoparticles.
A very high purity of the produced HAP material resulted from the IR analyses made by the IR instrument model PW1830 supplied by Philips. A typical IR diagram is reported in Fig.3 where we may notice a perfect correspondence between the peaks relevant to the obtained material and those characteristic of HAP.

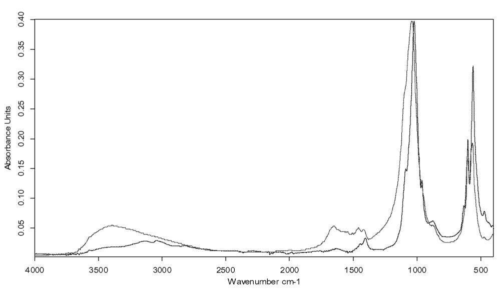

Figure 3: IR analysis of the produced HAP material

For each run, the following parameters were determined by means of the developed model: the layer thickness of the solution in the point of injection of the reagents, $\delta_{1,2}$; the Reynolds number in the point of injection of the reagents $Re_{1,2}$; the specific power in the point of injection of the reagents, $\varepsilon_{1,2}$; the residence time on the disk from the point of injection of the reagents, τ; the mixing time, t_{mix}; the average radial velocity in the point of injection of the reagents, $\bar{v}_{1,2}$; the micromixing length expressed by eq. (11), λ. The obtained results are reported in Tab. 1.
We may observe that the mixing time for every configuration is smaller than 1 ms and the Kolmogorov micromixing scale is lower than 10 μm. These conditions are characteristics of the attainment of micromixing between the reagents, which assure a mixing time smaller than the nucleation induction time, expected equal or greater than 1 ms. The average size of the particles in the three different cases is determined by both the number of nanoparticles locally generated and their aggregation grade due to the particles collisions under a residual supersaturation. If we assume that in any case we have the same number of generated nanoparticles, the remarkable increase of the particles size for an injection at 5 cm from the centre is mainly due to a higher

aggregation rate. This fact is justified by the lower Reynolds number and lower radial velocity which enhance the probability of particles collisions. Recently Bhatelia et al (2009) made a 3D simulation of a liquid layer over an RDR 3.5 cm in diameter and showed that there is a waveless laminar regime in the initial section followed by asymmetric wave formation, turbulent region and a second laminar-wave region near the outer perimeter. The injections zone corresponding to the first two cases, examined in this work, should be, thus, characterized by the presence of asymmetric waves which leads to a further reduction of the particles collisions.

5. Conclusions

The continuous production of nanoparticles of HAP, that is smaller than 100 nm in size, is possible by using a RDR and by optimizing the location of the feed points of the reagents. In fact, in this work HAP nanoparticles down to 58 nm in size were produced. A simplified model developed to predict the hydrodynamics of the liquid over the disc and the specific energy dispersion map was successfully used for the interpretation of the experimental results. However, for this purpose a more rigorous model based on the CFD technique could be useful. Finally, it has to be noticed that the applied reaction conditions together with the subsequent washing of the produced nanoparticles allowed to produce HAP material of high purity.

References

Balasundaram G., Sato M., Webster T.J., 2006, Using hydroxyapatite nanoparticles and decreased crystallinity to promote osteoblast adhesion similar to functionalizing with RGD, Biomaterials 27, 2798–2805.

Baldyga, J. and Bourne, J.R., 1984, A fluid mechanical approach to turbulent mixing and chemical reaction: Micromixing in the light of turbulence theory, Chem. Eng. Commun., 28, 243-258.

Bhatelia, T.J., Utikar, R.P., Pareek, V.K. and Tade, O.M., 2009, Characterizing liquid film thickness in spinning disc reactors, Proceedings of the Seventh International Conference on CFD in the Minerals and Process Industries, CSIRO, Melbourne, Australia, 9-11 December 2009.

Bird R.B., Stewart W.E., Lightfoot E.N., 1960, Transport Phenomena, Wiley & Sons, New York.

Brauer H., 1958, Stoffaustausch beim Rieselfilm, Chem. Ing. Tech, 30 (2), 75 -84.

Cafiero M.L., Baffi G., Chianese A., Jachuck R., 2002, Process Intensification: Precipitation of Barium Sulphate Using a Rotating Disk Reactor (RDR), Industrial Engineering Chemistry Research 41, 5240-46.

Moore, S. R., 1996, Mass Transfer to Thin Liquid Films on Rotating Surfaces, with and without Chemical Reaction, Ph.D. Dissertation, University of Newcastle upon Tyne, Newcastle upon Tyne, U.K.

Stoller M., Miranda L., Chianese A., 2009, Optimal feed location in a rotating disk reactor for the production of TiO2 nanoparticles, Chemical Engineering Transactions 17, 993-998.